Stable wrench-feasible workspace of a 2-X tensegrity manipulator

Vimalesh Muralidharan

Stable wrench-feasible workspace of a 2-X tensegrity manipulator

Vimalesh Muralidharan

Laboratoire des Sciences du Numérique de Nantes (LS2N), CNRS, 44321 Nantes, France {Vimalesh.Muralidharan@ls2n.fr}

Abstract

The stable wrench-feasible workspace (SWFW) of a cable-driven tensegrity manipulator defines the set of all end-effector poses reachable with a stable equilibrium configuration, for a positive and bounded input cable forces. A method for determining the boundary points of the SWFW of a manipulator with two anti-parallelogram (X) joints and link offsets, actuated remotely by four cables, has been proposed. It involves two 1-dimensional (D) scanning of the joint space to firstly determine the bounding points of the stable wrench-feasible joint space (SWFJ), followed by those of the SWFW. At each grid in the joint space, a set of univariate polynomial equations are solved to determine the desired boundary points with a good accuracy. The steps involved in the derivation of two of these polynomials are detailed, while the others are also derived in a similar manner. Finally, a numerical example of the 2-X manipulator is considered and its SWFW boundary points are visualized.

1 Introduction

Figure 1 shows the schematic of a 2-X manipulator composed of two anti-parallelogram (X) joints and link offsets. Each joint consists of a top and a base bar of length b, and two crossed bars of length l, with $(l > b)$ for the assembly of the joints. The orientation of the top bar w.r.t. the base bar of i^{th} joint is given by α_i for $i = 1, 2$. Each joint is composed of identical springs with stiffness k_i on either sides, to ensure that it remains in equilibrium at $\alpha_i = 0$, in the absence of external forces. There is a rigid offset of length a between the two joints, and between the second joint and the end-effector point $P(x, y)$.

The range of motion of each X-joint is limited by $-\pi < \alpha_i < \pi$, due to the flat-singularities at $\alpha_i = \pm\pi$ (see [1]). Within this range, each joint is independently actuated by two cables C_{l_i}, C_{r_i} in an antagonistic manner as shown in Fig. 2b. Each of these cables are actuated by a motor fixed at

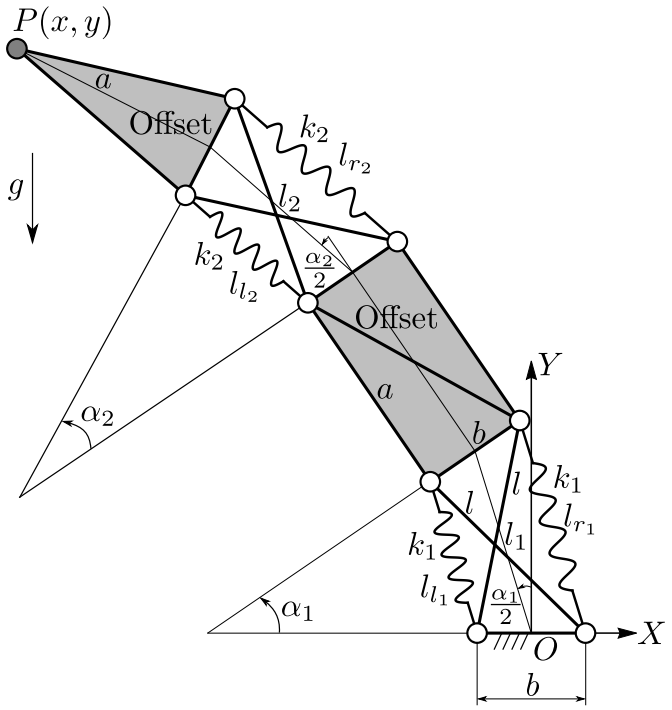

Figure 1: Schematic of the 2-X manipulators under study.

the base. The cables C_{l_2}, C_{r_2} have been routed along the bars of the first joint and the offset in a strut-routed scheme (see [1]) with pulleys, so as to preserve the independence in actuation. In this study, the springs are assumed to be of zero-free length and the pulleys to be massless points.

The kinematic model of 2-X manipulator, involves expressing the end-effector coordinates (x, y) in terms of the joint angles (α_1, α_2) and vice versa. From Fig. 1, knowing that $\alpha_i \in]-\pi, \pi[, i = 1, 2$, it is possible to *unambiguously* present the direct kinematics of the manipulator as follows (see [2] for details):

$$\begin{cases} l_i(\alpha_i) = \sqrt{l^2 - b^2\cos^2(\alpha_i/2)}, \quad i = 1, 2 \\ x = -l_1(\alpha_1)\sin(\alpha_1/2) - a(\sin\alpha_1 + \sin(\alpha_1+\alpha_2)) - l_2(\alpha_2)\sin(\alpha_1+\alpha_2/2) \\ y = l_1(\alpha_1)\cos(\alpha_1/2) + a(\cos\alpha_1 + \cos(\alpha_1+\alpha_2)) + l_2(\alpha_2)\cos(\alpha_1+\alpha_2/2) \end{cases} \tag{1}$$

Differentiating Eq. (1) w.r.t. time yields :

$$\begin{pmatrix} \dot{x} \\ \dot{y} \end{pmatrix} = \boldsymbol{J}_x \begin{pmatrix} \dot{\alpha}_1 \\ \dot{\alpha}_2 \end{pmatrix}, \text{where } \boldsymbol{J}_x = \begin{pmatrix} \frac{\partial x}{\partial \alpha_1} & \frac{\partial x}{\partial \alpha_2} \\ \frac{\partial y}{\partial \alpha_1} & \frac{\partial y}{\partial \alpha_2} \end{pmatrix} \text{is a Jacobian matrix.} \tag{2}$$

The singularity condition for the manipulator is obtained from the vanishing of the determinant

of $\boldsymbol{J}_x$, which can be expressed as follows (after clearing the non-zero denominator):

$$\begin{aligned}
&4a\sin\alpha_{22}\sqrt{l^2-b^2\cos^2\alpha_{22}}\left(l^2-2b^2\cos^2\alpha_{22}\right)+2b^4\cos\alpha_{12}\sin\alpha_{22}\cos^2\alpha_{22}\\
&+b^2l^2\left(\sin(\alpha_{12}-\alpha_{22})-2\cos^2\alpha_{22}\sin(\alpha_{12}+\alpha_{22})\right)+l^4\sin(\alpha_{12}+\alpha_{22})\\
&+\sqrt{l^2-b^2\cos^2\alpha_{22}}\left(2a\left(\cos\alpha_{12}\sin\alpha_2\left(l^2-b^2\right)-l^2\sin\alpha_{12}\sin^2\alpha_{22}+l^2\sin\alpha_{12}\cos^2\alpha_{22}\right)\right.\\
&\left.-\left(b^2-4a^2\right)\sin\alpha_2\sqrt{l^2-b^2\cos^2\alpha_{12}}\right)=0
\end{aligned} \tag{3}$$

where $\alpha_{12}=\alpha_1/2, \alpha_{22}=\alpha_2/2$. Such substitutions have been made above and in the rest of this document, for the sake of brevity. Note that $(\alpha_1,\alpha_2)=(0,0)$ satisfies the singularity condition irrespective of the bar lengths.

2 Static model of the 2-X manipulator

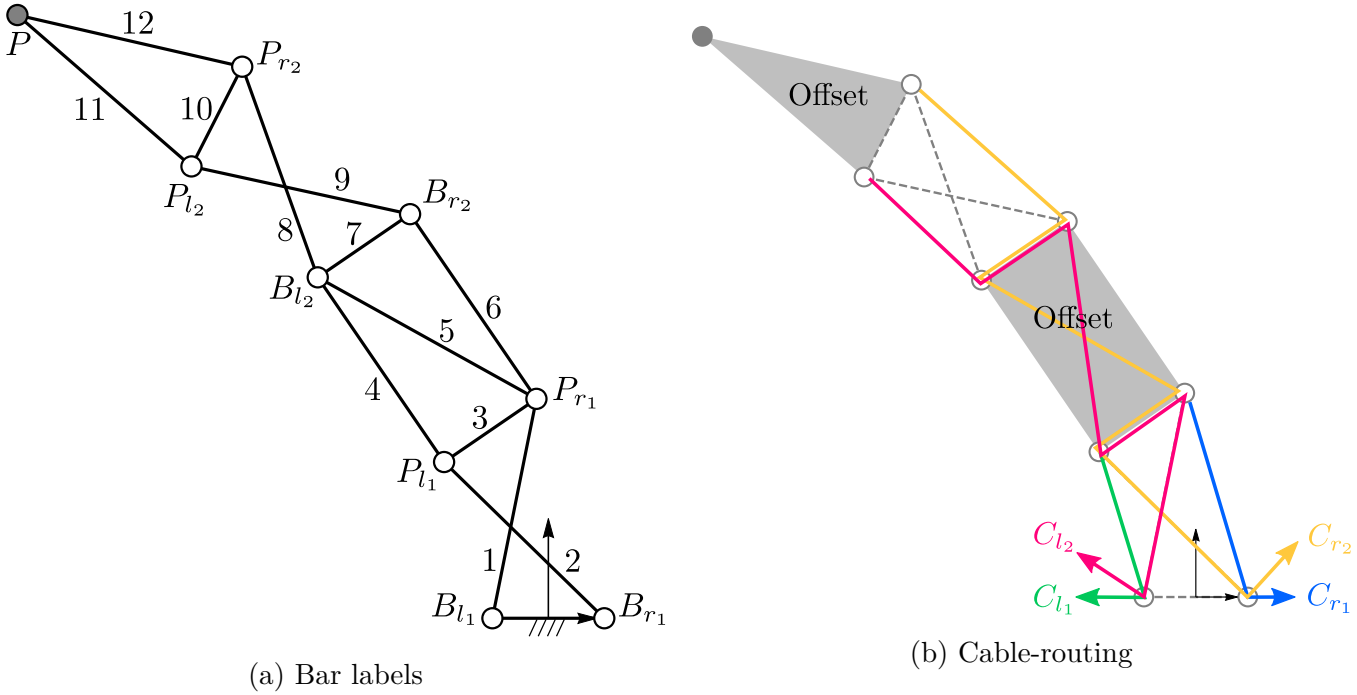

(a) Bar labels

(b) Cable-routing

Figure 2: Bar labels (left) and cable-routing scheme (right) for the 2-X manipulator.

The total potential energy of the 2-X manipulator is computed as follows:

$$U_x=\sum_{i=1}^{12}m_igy_i+m_pgy_p+\sum_{j=1}^{2}(1/2)k_j(l_{l_j}^2+l_{r_j}^2)+F_{l_j}l_{l_j}+F_{r_j}l_{r_j} \tag{4}$$

where m_i represents the mass of the i^{th} bar (see Fig. 2a), y_i represents the y-coordinate of the geometric center of the bar i, m_p is the mass of the point payload and y_p its y-coordinate. Together the first two terms represent the contribution of gravity in the total potential energy (considering

the zero-potential to be along the x-axis). The remaining terms signify the effect of springs and actuation forces. The lengths l_{l_j}, l_{r_j}, shown in Fig. 1, are functions of l, b, α_j (see [3] for their expressions). The forces F_{l_j}, F_{r_j} are the actuation forces imposed by cables C_{l_j}, C_{r_j} (see Fig. 2b), respectively, with $j = 1, 2$.

The static equilibrium equations can be obtained by setting the derivatives of U_x w.r.t. α_1 and α_2, to zeros. This results in two equations, which can written in the following form[1]:

$$\begin{cases} G_1(k_1, g, l, b, \alpha_1, \alpha_2) = \Gamma_1(F_{l_1}, F_{r_1}, l, b, \alpha_1) \\ G_2(k_2, g, l, b, \alpha_1, \alpha_2) = \Gamma_2(F_{l_2}, F_{r_2}, l, b, \alpha_2) \end{cases} \tag{5}$$

$$\begin{cases} G_1 = C_{1x}\sin\alpha_1 - C'_{3x}\sin(\alpha_1+\alpha_2) - 2C_{3x}\sin(\alpha_1+\alpha_{22})\sqrt{l^2 - b^2\cos^2\alpha_{22}} + \frac{C'_{1x}\sin\alpha_{12}\left(2b^2\cos^2\alpha_{12} - l^2\right)}{\sqrt{l^2 - b^2\cos^2\alpha_{12}}} \\ G_2 = \frac{C_{3x}\left(b^2\sin\alpha_{22}\cos(\alpha_1+\alpha_{22})\cos\alpha_{22} + \sin(\alpha_1+\alpha_{22})\left(b^2\cos^2\alpha_{22} - l^2\right)\right)}{\sqrt{l^2 - b^2\cos^2\alpha_{22}}} + C_{2x}\sin\alpha_2 - C'_{3x}\sin(\alpha_1+\alpha_2) \\ \Gamma_1 = -F_{l_1} b\cos\alpha_{12}\left(\frac{b\sin\alpha_{12}}{\sqrt{l^2 - b^2\cos^2\alpha_{12}}} - 1\right) - F_{r_1} b\cos\alpha_{12}\left(\frac{b\sin\alpha_{12}}{\sqrt{l^2 - b^2\cos^2\alpha_{12}}} + 1\right) \\ \Gamma_2 = -F_{l_2} b\cos\alpha_{22}\left(\frac{b\sin\alpha_{22}}{\sqrt{l^2 - b^2\cos^2\alpha_{22}}} - 1\right) - F_{r_2} b\cos\alpha_{22}\left(\frac{b\sin\alpha_{22}}{\sqrt{l^2 - b^2\cos^2\alpha_{22}}} + 1\right) \end{cases} \tag{6}$$

where

$$\begin{cases} C_{1x} = 2b^2k_1 - ag(2m_{10} + 4m_{11} + m_3 + 2m_4 + m_5 + m_7 + 4m_8 + 2m_p) \\ C'_{1x} = g(m_1 + m_{10} + 2m_{11} + m_3 + 2m_4 + m_5 + m_7 + 2m_8 + m_p) \\ C_{2x} = 2b^2k_2 \\ C_{3x} = g(m_{10} + 2m_{11} + m_8 + m_p) \\ C'_{3x} = 2ag(m_{11} + m_p) \end{cases} \tag{7}$$

The masses (m_2, m_6, m_9, m_{12}) have been replaced by (m_1, m_4, m_8, m_{11}), respectively, owing to symmetry (see Fig. 2a) to keep the resulting expressions simpler.

The coefficients of F_{l_i} (resp. F_{r_i}) can be shown to be positive (resp. negative) within the range $-\pi < \alpha_i < \pi$. Thus, when the cable forces are bounded by $[F_{\min}, F_{\max}]$, the maximum (resp. minimum) values of the actuation wrench Γ_i can be obtained when $\overline{\Gamma_i}(F_{l_i} = F_{\max}, F_{r_i} = F_{\min})$ (resp. $\underline{\Gamma_i}(F_{l_i} = F_{\min}, F_{r_i} = F_{\max})$). Thus, the equilibrium equations in Eq. (5) can be satisfied only when $\underline{\Gamma_i} \leq G_i \leq \overline{\Gamma_i}$. The set of all $\alpha_i \in]-\pi, \pi[$ where these inequalities are satisfied forms the wrench-feasible joint space (WFJ) of the manipulator. The boundary of WFJ will be obtained from the conditions $G_i = \underline{\Gamma_i}$ and $G_i = \overline{\Gamma_i}$.

[1]The symbol g in Eq. (5) represents all the terms due to gravity.

The articular stiffness matrix ($\boldsymbol{K}_\alpha$) of the 2-X manipulator is obtained from the Hessian of the potential energy w.r.t. $[\alpha_1, \alpha_2]^\top$, as follows:

$$\boldsymbol{K}_\alpha = \begin{pmatrix} K_{11} & K_{12} \\ K_{12} & K_{22} \end{pmatrix} \text{ with } K_{11} = \frac{K_{11}^{'}}{(\lambda^2 - c_1^2)^{3/2}} \text{ and } K_{22} = \frac{K_{22}^{'}}{(\lambda^2 - c_2^2)^{3/2}} \tag{8}$$

where

$$\begin{aligned} K_{11}^{'} = & -4bc_{12}C_{3x}\left(\lambda^2 - c_1^2\right)^{3/2}\sqrt{\lambda^2 - c_2^2} - bc_1C_{1x}^{'}\left(4c_1^4 - 2c_1^2\left(3\lambda^2 + 1\right) + \lambda^2\left(\lambda^2 + 3\right)\right) \\ & - bF_{l_1}\left(c_1^4 + c_1^2\left(s_1\sqrt{\lambda^2 - c_1^2} - \lambda^2\right) + \lambda^2 s_1\left(s_1 - \sqrt{\lambda^2 - c_1^2}\right)\right) \\ & - bF_{r_1}\left(c_1^4 - c_1^2\left(s_1\sqrt{\lambda^2 - c_1^2} + \lambda^2\right) + \lambda^2 s_1\left(\sqrt{\lambda^2 - c_1^2} + s_1\right)\right) \\ & - 2c_{12}^{'}C_{3x}^{'}\left(\lambda^2 - c_1^2\right)^{3/2} + 2C_{1x}\left(\lambda^2 - c_1^2\right)^{3/2}\left(c_1^2 - s_1^2\right) \end{aligned} \tag{9}$$

$$\begin{aligned} K_{22}^{'} = & C_{3x}\left(bc_{12}\left(-2c_2^4 + 3c_2^2\lambda^2 - \lambda^2\left(\lambda^2 + s_2^2\right)\right) + 2bc_2s_{12}s_2\left(c_2^2 - \lambda^2\right)\right) \\ & - bF_{l_2}\left(c_2^4 + c_2^2\left(s_2\sqrt{\lambda^2 - c_2^2} - \lambda^2\right) + \lambda^2 s_2\left(s_2 - \sqrt{\lambda^2 - c_2^2}\right)\right) \\ & - bF_{r_2}\left(c_2^4 - c_2^2\left(s_2\sqrt{\lambda^2 - c_2^2} + \lambda^2\right) + \lambda^2 s_2\left(\sqrt{\lambda^2 - c_2^2} + s_2\right)\right) \\ & - 2c_{12}^{'}C_{3x}^{'}\left(\lambda^2 - c_2^2\right)^{3/2} + 2C_{2x}\left(\lambda^2 - c_2^2\right)^{3/2}\left(c_2^2 - s_2^2\right) \end{aligned} \tag{10}$$

$$K_{12} = -\frac{2bC_{3x}\left(c_{12}\left(\lambda^2 - c_2^2\right) + c_2s_{12}s_2\right)}{\sqrt{\lambda^2 - c_2^2}} - 2c_{12}^{'}C_{3x}^{'} \tag{11}$$

in which $\lambda = l/b$, $c_1 = \cos(\alpha_1/2), s_1 = \sin(\alpha_1/2), c_2 = \cos(\alpha_2/2), s_2 = \sin(\alpha_2/2), c_{12} = \cos(\alpha_1 + \alpha_2/2), s_{12} = \sin(\alpha_1 + \alpha_2/2), c_{12}^{'} = \cos(\alpha_1 + \alpha_2), s_{12}^{'} = \sin(\alpha_1 + \alpha_2)$.

At any given configuration (α_1, α_2), the manipulator is said to be at a stable equilibrium if two conditions are satisfied. Firstly, the equilibrium equations in Eq. 5 must be satisfied, and secondly, the matrix $\boldsymbol{K}_\alpha$ must be positive definite. To satisfy the first condition, two of the forces, e.g., (F_{l_1}, F_{l_2}) can be solved for from Eq. (5) and substituted into the stiffness matrix. This results in the matrix $\boldsymbol{K}_\alpha^{\mathrm{rr}}$, given below:

$$\boldsymbol{K}_\alpha^{\mathrm{rr}} = \begin{pmatrix} K_{11}^{\mathrm{rr}} & K_{12} \\ K_{12} & K_{22}^{\mathrm{rr}} \end{pmatrix} \text{ with } K_{11}^{\mathrm{rr}} = \frac{K_{11}^{\mathrm{rr}'}}{c_1(\lambda^2 - c_1^2)} \text{ and } K_{22}^{\mathrm{rr}} = \frac{K_{22}^{\mathrm{rr}'}}{c_2(\lambda^2 - c_2^2)} \tag{12}$$

where

$$\begin{aligned} K_{11}^{\mathrm{rr}'} = & -2bC_{3x}\sqrt{\lambda^2 - c_2^2}\left(2c_1c_{12}\left(\lambda^2 - c_1^2\right) + c_1^2s_{12}\sqrt{\lambda^2 - c_1^2} + \lambda^2 s_1 s_{12}\right) \\ & + C_{1x}^{'}\left(bc_1^2s_1\left(2c_1^2 - \lambda^2\right) + b\left(4c_1^4 - 2c_1^2 - \lambda^2\right)\sqrt{\lambda^2 - c_1^2}\right) + 2bc_1^3F_{r_1}\left(\sqrt{\lambda^2 - c_1^2} + s_1\right) \\ & + C_{3x}^{'}\left(2c_1c_{12}^{'}\left(c_1^2 - \lambda^2\right) + c_1^2(-s_{12}^{'})\sqrt{\lambda^2 - c_1^2} - \lambda^2 s_1 s_{12}^{'}\right) + 2c_1^3C_{1x}\left(s_1\sqrt{\lambda^2 - c_1^2} - c_1^2 + \lambda^2 + s_1^2\right) \end{aligned} \tag{13}$$

$$K_{22}^{\mathrm{rr}'} = C_{3x}\left(bc_{12}\left(c_2^3\left(2\sqrt{\lambda^2-c_2^2}+s_2\right)-c_2\lambda^2\sqrt{\lambda^2-c_2^2}\right)\right.$$
$$\left.+\,bs_{12}\left(c_2^4-c_2^2\left(2s_2\sqrt{\lambda^2-c_2^2}+\lambda^2\right)-\lambda^2 s_2\sqrt{\lambda^2-c_2^2}\right)\right)+2bc_2^3F_{r_2}\left(\sqrt{\lambda^2-c_2^2}+s_2\right)$$
$$+\,C_{3x}'\left(2c_{12}'c_2\left(c_2^2-\lambda^2\right)+s_{12}'\left(c_2^2\left(-\sqrt{\lambda^2-c_2^2}\right)-\lambda^2 s_2\right)\right)+2c_2^3C_{2x}\left(s_2\sqrt{\lambda^2-c_2^2}-c_2^2+\lambda^2+s_2^2\right) \tag{14}$$

Recalling that $(l > b)$ (or $\lambda > 1$) and $\alpha_i \in \,]-\pi, \pi[\,, i = 1, 2$, it can be shown that the coefficients of F_{r_1} and F_{r_2} are both positive. This shows that the actuation forces have a positive influence on the stiffness of the 2-X manipulator.

Thus, at a given configuration (α_1, α_2), maximum stiffness can be obtained by imposing maximum feasible values for (F_{r_1}, F_{r_2}). They can be set to $F_{\max}$ each, if the corresponding (F_{l_1}, F_{l_2}) computed from the equilibrium equations are both within $[F_{\min}, F_{\max}]$. If this is not the case, then F_{l_i} must be set to $F_{\max}$ and the respective values of F_{r_i} must be determined from the i^{th} equilibrium equation.

In general, two of the actuation forces $\{(F_{r_1}, F_{r_2})$ or (F_{r_1}, F_{l_2}) or (F_{l_1}, F_{r_2}) or $(F_{l_1}, F_{l_2})\}$ must be set to their upper bound of $F_{\max}$ to obtain maximum stiffness at any configuration. However, while determining the stability boundary one does not know a priori which combination of forces is the critical one. Hence, the stiffness matrices corresponding to all the above force combinations must be obtained: $(\boldsymbol{K}_\alpha^{\mathrm{rr}}, \boldsymbol{K}_\alpha^{\mathrm{rl}}, \boldsymbol{K}_\alpha^{\mathrm{lr}}, \boldsymbol{K}_\alpha^{\mathrm{ll}})$, respectively, by eliminating the other two forces using the equilibrium equations. Then, the forces in each of these matrices must be set to $F_{\max}$ to form the matrices corresponding to maximum stiffness $(\overline{\boldsymbol{K}}_\alpha^{\mathrm{rr}}, \overline{\boldsymbol{K}}_\alpha^{\mathrm{rl}}, \overline{\boldsymbol{K}}_\alpha^{\mathrm{lr}}, \overline{\boldsymbol{K}}_\alpha^{\mathrm{ll}})$, respectively. The boundary of stability could be formed by the vanishing of the determinant of any of these matrices[2]. Hence, all of these conditions must be considered together for determining the stability boundary in the joint space.

The set of all (α_1, α_2) where the manipulator is both wrench-feasible and stable forms the stable wrench-feasible joint space (SWFJ). A method to compute its bounding points is presented in the following.

[2]Normally the positive definiteness of a (2×2) matrix is ensured when both of its leading principal minors are positive. But, for real symmetric matrices it can be shown that the boundary (limiting case) of positive definiteness can only be formed by the vanishing of the second leading minor (see Appendix A)

3 Boundary points of the SWFJ

As a first step in the determination of the SWFJ boundary, all the limiting conditions of wrench-feasibility and stability can be grouped together as follows:

$$\boldsymbol{f}(\alpha_1, \alpha_2) := \begin{cases} f_1 := G_1 - \underline{\Gamma_1} = 0 \\ f_2 := -G_1 + \overline{\Gamma_1} = 0 \\ f_3 := G_2 - \underline{\Gamma_2} = 0 \\ f_4 := -G_2 + \overline{\Gamma_2} = 0 \\ f_5 := \det(\overline{\boldsymbol{K}}_{\alpha}^{\mathrm{rr}}) = 0 \\ f_6 := \det(\overline{\boldsymbol{K}}_{\alpha}^{\mathrm{rl}}) = 0 \\ f_7 := \det(\overline{\boldsymbol{K}}_{\alpha}^{\mathrm{lr}}) = 0 \\ f_8 := \det(\overline{\boldsymbol{K}}_{\alpha}^{\mathrm{ll}}) = 0 \end{cases} \tag{15}$$

It is possible to plot the contours of the above expressions in (α_1, α_2) space and determine the SWFJ by inspecting the feasibility of one point inside each connected region. However, this approach requires manual intervention and is not suitable for a design process, where thousands of manipulator designs might be explored.

Hence, an alternate approach is followed in this work. Each of the above conditions can be converted to a polynomial in tangent half-angle of the joint angles, say α_1, by retaining α_2 in its coefficients. Thus, for a given α_2, it would be possible to obtain the limiting values of α_1 from all the equations in Eq. (15). Then, one point inside each interval can be explored to determine the feasibility of that interval. The bounding points of the feasible intervals of α_1 would lie on the boundary of SWFJ. Thus, α_2 may be discretized at a desired resolution and the respective bounding points in α_1 may be obtained.

This process can be repeated by deriving polynomials in half-tangent form of α_2, and solving them at discrete values of α_1, to obtain the bounding points of α_2. In this manner, a cloud of points that lie on the SWFJ boundary can be determined and then mapped onto the task space along with the singularities using the direct kinematic equations, to obtain the SWFW.

The steps involved in the derivation of these polynomials are illustrated for the first condition in Eq. (15) in the next section.

4 Equivalent polynomial equations for $f_1 = 0$

Using the expressions in Eq. (6), the equation $f_1 = 0$ in Eq. (15) can be expanded into:

$$\begin{aligned} & b\cos\left(\frac{\alpha_1}{2}\right)(F_{\max} - F_{\min}) + C_{1x}\sin\alpha_1 - C'_{3x}\sin(\alpha_1+\alpha_2) \\ & + \frac{b^2\sin\left(\frac{\alpha_1}{2}\right)\left(C'_{1x}\left(\cos(\alpha_1) - \lambda^2 + 1\right) + \cos\left(\frac{\alpha_1}{2}\right)(F_{\max}+F_{\min})\right)}{\sqrt{l^2 - b^2\cos^2\left(\frac{\alpha_1}{2}\right)}} \\ & + -2bC_{3x}\sin\left(\alpha_1 + \frac{\alpha_2}{2}\right)\sqrt{\lambda^2 - \cos^2\left(\frac{\alpha_2}{2}\right)} = 0 \end{aligned} \tag{16}$$

This condition would be processed differently to obtain polynomials in $t_1 = \tan(\alpha_1/4)$ and $\tan(\alpha_2/4)$, respectively, in the following sections.

4.1 Polynomial in $t_1 = \tan(\alpha_1/4)$

The objective is to rewrite $f_1 = 0$ as a polynomial in $t_1 = \tan(\alpha_1/4)$. In this case, α_2 and all other parameters are assumed to be known. Starting from Eq. (16), the trigonometric terms with compound angles are expanded and the substitutions $c_2 = \cos(\alpha_2/2), s_2 = \sin(\alpha_2/2)$ are carried out. The next step is to eliminate the square root involving α_1. Hence, this equation is rewritten in terms of intermediate variables (for simplicity and fast computations) as follows:

$$\begin{aligned} & b^2\sin(\alpha_1/2)\left(aa_4\cos(\alpha_1/2) + C'_{1x}\left(2\cos^2(\alpha_1/2) - \lambda^2\right)\right)\frac{1}{\sqrt{l^2 - b^2\cos^2(\alpha_1/2)}} \\ & = \cos(\alpha_1/2)(aa_1\sin(\alpha_1/2) + aa_3) + aa_2\cos\alpha_1 \end{aligned} \tag{17}$$

$$\begin{cases} aa_1 = -4bc_2C_{3x}\sqrt{\lambda^2 - c_2^2} + 2C_{1x} - 2c_2^2C'_{3x} + 2C'_{3x}s_2^2 \\ aa_2 = -2s_2\left(bC_{3x}\sqrt{\lambda^2 - c_2^2} + c_2C'_{3x}\right) \\ aa_3 = b(F_{\max} - F_{\min}) \\ aa_4 = F_{\max} + F_{\min} \end{cases} \tag{18}$$

Squaring both sides of Eq. (17) and clearing the denominator($\neq 0$) results in:

$$\begin{aligned} & b^4\sin^2(\alpha_1/2)\left(aa_4\cos(\alpha_1/2) + C'_{1x}\left(2\cos^2(\alpha_1/2) - \lambda^2\right)\right)^2 \\ & - \left(b^2\lambda^2 - b^2\cos^2(\alpha_1/2)\right)\left(\cos(\alpha_1/2)(aa_1\sin(\alpha_1/2) + aa_3) + aa_2\left(2\cos^2(\alpha_1/2) - 1\right)\right)^2 = 0 \end{aligned} \tag{19}$$

Though spurious roots will be introduced due to squaring, they will be eliminated automatically, in the next step while inspecting the intervals (see Fig. 3a). Introducing the variable $t_1 = \tan\left(\frac{\alpha_1}{4}\right)$,

and replacing: $\cos(\alpha_1/2) = \frac{1-t_1^2}{1+t_1^2}$ and $\sin(\alpha_1/2) = \frac{2t_1}{1+t_1^2}$, results in a rational equation. After clearing the non-zero denominator $(1+t_1^2)^6$, one obtains a degree-12 polynomial as follows:

$$\zeta_0 + \zeta_1 t_1 + \zeta_2 t_1^2 + \zeta_3 t_1^3 + \zeta_4 t_1^4 + \zeta_5 t_1^5 + \zeta_6 t_1^6 + \zeta_7 t_1^7 + \zeta_8 t_1^8 + \zeta_9 t_1^9 + \zeta_{10} t_1^{10} + \zeta_{11} t_1^{11} + \zeta_{12} t_1^{12} = 0 \quad (20)$$

$$\begin{cases}
\zeta_0 = b^2\left(\lambda^2-1\right)\left(-(aa_2+aa_3)^2\right) \\
\zeta_1 = -4aa_1b^2\left(\lambda^2-1\right)\left(aa_2+aa_3\right) \\
\zeta_2 = -2b^2\left(2aa_1^2\left(\lambda^2-1\right)+aa_2^2\left(7-5\lambda^2\right)-4aa_2aa_3\left(\lambda^2-2\right)+aa_3^2\lambda^2+aa_3^2-2aa_4^2b^2\right. \\
\qquad \left.+4aa_4b^2C'_{1x}\lambda^2-8aa_4b^2C'_{1x}-2b^2\left(C'_{1x}\right)^2\lambda^4+8b^2(C'_{1x})^2\lambda^2-8b^2(C'_{1x})^2\right) \\
\zeta_3 = -4aa_1b^2\left(aa_2\left(9-5\lambda^2\right)+aa_3\left(\lambda^2+3\right)\right) \\
\zeta_4 = -b^2\left(16aa_1^2+3aa_2^2\left(5\lambda^2-21\right)-2aa_2aa_3\left(11\lambda^2+13\right)-aa_3^2\lambda^2+aa_3^2+16aa_4b^2C'_{1x}\lambda^2\right. \\
\qquad \left.+32aa_4b^2C'_{1x}-16b^2\left(C'_{1x}\right)^2\lambda^4+64b^2\left(C'_{1x}\right)^2\right) \\
\zeta_5 = 8aa_1b^2\left(3aa_2\lambda^2+11aa_2+aa_3\lambda^2+aa_3\right) \\
\zeta_6 = 4b^2\left(2aa_1^2\left(\lambda^2+3\right)-aa_2^2\left(13\lambda^2+25\right)+aa_3^2\lambda^2+aa_3^2-2aa_4^2b^2+6b^2\left(C'_{1x}\right)^2\lambda^4\right. \\
\qquad \left.+8b^2\left(C'_{1x}\right)^2\lambda^2+24b^2\left(C'_{1x}\right)^2\right) \\
\zeta_7 = 8aa_1b^2\left(-3aa_2\lambda^2-11aa_2+aa_3\lambda^2+aa_3\right) \\
\zeta_8 = b^2\left(-16aa_1^2+aa_2^2\left(63-15\lambda^2\right)-2aa_2aa_3\left(11\lambda^2+13\right)+aa_3^2\lambda^2-aa_3^2+16aa_4b^2C'_{12}\lambda^2\right. \\
\qquad \left.+32aa_4b^2C'_{12}+16b^2\left(C'_{12}\right)^2\lambda^4-64b^2\left(C'_{12}\right)^2\right) \\
\zeta_9 = -4aa_1b^2\left(aa_2\left(5\lambda^2-9\right)+aa_3\left(\lambda^2+3\right)\right) \\
\zeta_{10} = -2b^2\left(2aa_1^2\left(\lambda^2-1\right)+aa_2^2\left(7-5\lambda^2\right)+4aa_2aa_3\left(\lambda^2-2\right)+aa_3^2\lambda^2+aa_3^2-2aa_4^2b^2\right. \\
\qquad \left.-4aa_4b^2C'_{12}\lambda^2+8aa_4b^2C'_{12}-2b^2\left(C'_{12}\right)^2\lambda^4+8b^2\left(C'_{12}\right)^2\lambda^2-8b^2\left(C'_{12}\right)^2\right) \\
\zeta_{11} = 4aa_1b^2\left(\lambda^2-1\right)\left(aa_2-aa_3\right) \\
\zeta_{12} = b^2\left(\lambda^2-1\right)\left(-(aa_2-aa_3)^2\right)
\end{cases} \quad (21)$$

The above coefficients are functions of α_2, and will be known as numbers when the manipulator parameters and α_2 are known.

4.2 Polynomial in $t_2 = \tan(\alpha_2/4)$

Incorporating the substitutions $c_1 = \cos(\alpha_1/2), s_1 = \sin(\alpha_1/2)$ into Eq. (16), and rearranging it, results in:

$$ba_1\cos(\alpha_{22}) + ba_2\sin(\alpha_{22})\sqrt{\lambda^2-\cos^2(\alpha_2/2)} = ba_3 + ba_4\cos(\alpha_2) + ba_5\sin(\alpha_2) \quad (22)$$

where

$$\begin{cases} ba_1 = -4c_1 C_{3x} s_1 \\ ba_2 = 2C_{3x}(s_1^2 - c_1^2) \\ ba_3 = -\frac{bC'_{12}s_1\left(-3c_1^2+2\lambda^2+s_1^2-1\right)}{2\sqrt{\lambda^2-c_1^2}} + bc_1\left(\frac{F_{\max}s_1}{\sqrt{\lambda^2-c_1^2}} + F_{\min}\left(\frac{s_1}{\sqrt{\lambda^2-c_1^2}} - 1\right) + F_{\max}\right) + 2c_1 C_{1x} s_1 \\ ba_4 = -2c_1 C'_{3x} s_1 \\ ba_5 = -C'_{3x}(c_1^2 - s_1^2) \end{cases} \tag{23}$$

Squaring both sides to eliminate the square root leads to:

$$\left(b^2\lambda^2 - b^2\cos^2(\alpha_{22})\right)(ba_1\cos(\alpha_{22}) + ba_2\sin(\alpha_{22}))^2 - (ba_3 + ba_4\cos(\alpha_2) + ba_5\sin(\alpha_2))^2 = 0 \tag{24}$$

Introducing the variable $t_2 = \tan(\alpha_2/4)$, replacing $\cos(\alpha_2) = \frac{1-t_2^2}{1+t_2^2}$ and $\sin(\alpha_2/2) = \frac{2t_2}{1+t_2^2}$, and clearing the non-zero denominator $(1+t_2^2)^4$, one obtains:

$$\mu_0 + \mu_1 t_2 + \mu_2 t_2^2 + \mu_3 t_2^3 + \mu_4 t_1^4 + \mu_5 t_2^5 + \mu_6 t_2^6 + \mu_7 t_2^7 + \mu_8 t_2^8 = 0 \tag{25}$$

$$\begin{cases} \mu_0 = b^2 ba_1^2(\lambda^2-1) - (ba_3 + ba_4)^2 \\ \mu_1 = 4b^2 ba_1 ba_2(\lambda^2-1) - 8ba_5(ba_3 + ba_4) \\ \mu_2 = 4\left(b^2\left(ba_1^2 + ba_2^2(\lambda^2-1)\right) - ba_3^2 + 2ba_3 ba_4 + 3ba_4^2 - 4ba_5^2\right) \\ \mu_3 = 4b^2 ba_1 ba_2(\lambda^2+3) - 8ba_5(ba_3 - 7ba_4) \\ \mu_4 = b^2\left(8ba_2^2(\lambda^2+1) - 2ba_1^2(\lambda^2+3)\right) - 6ba_3^2 + 20ba_3 ba_4 - 38ba_4^2 + 32ba_5^2 \\ \mu_5 = 8ba_5(ba_3 - 7ba_4) - 4b^2 ba_1 ba_2(\lambda^2+3) \\ \mu_6 = 4\left(b^2\left(ba_1^2 + ba_2^2(\lambda^2-1)\right) - ba_3^2 + 2ba_3 ba_4 + 3ba_4^2 - 4ba_5^2\right) \\ \mu_7 = 8ba_5(ba_3 + ba_4) - 4b^2 ba_1 ba_2(\lambda^2-1) \\ \mu_8 = b^2 ba_1^2(\lambda^2-1) - (ba_3 + ba_4)^2 \end{cases} \tag{26}$$

Similar to previous case, all of these coefficients will be known as numbers when all the manipulator parameters and α_1 are known.

4.3 Details on other polynomials

Each of the conditions in Eq. (15) can be reduced to polynomials in $t_1 = \tan(\alpha_1/2), t_2 = \tan(\alpha_2/2)$, respectively, as illustrated in the previous two sections. The derivation of polynomials for the stability conditions involves more intermediate variables, bigger expressions, and more tedious computations. Each stability condition results in a polynomial of degree-36, which are not presented in this report due to lack of space. A total of 16 polynomials have been derived from Eq. (15), 8 of them in t_1 and the other 8 in t_2.

5 Boundary points of the SWFW for a numerical example

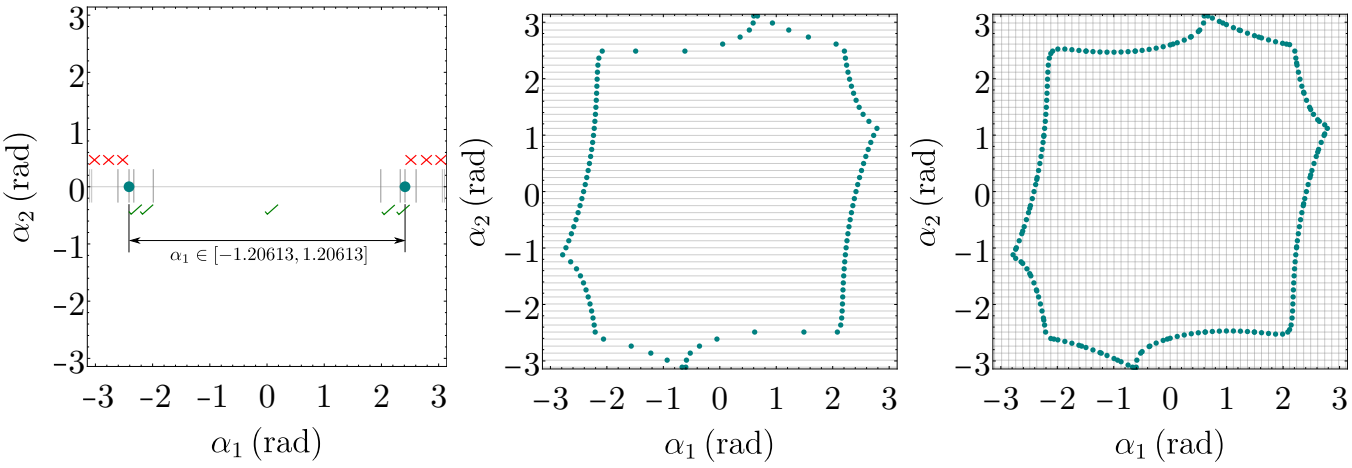

(a) Intervals of α_1 when $\alpha_2 = 0$

(b) Scanning α_2

(c) Scanning both α_1 and α_2

Figure 3: 2X manipulator: Feasible interval of α_1 for a given $\alpha_2 = 0$ (left), boundary points obtained while scanning α_2 (middle), and all the boundary points obtained by scanning both α_1 and α_2 (right).

For a numerical illustration, the following parameters have been adopted for the 2-X manipulator: $b = 0.05$ m, $l = 0.1$ m, $a = 0.2$ m, $k_1 = 600$ N/m, $k_2 = 300$ N/m. The forces imparted by all the cables are bounded between $F_{\min} = 5$ N and $F_{\max} = 155$ N. All the bars (thick lines in Fig. 2a) are considered to be made of Aluminum material as solid cylinders of radius 0.005 m.

For the 2-X manipulator, determination of the SWFJ involves two 1-D scans, i.e., of α_1, α_2 variables separately. They were each discretized into 50 equally spaced points inside $[-0.99\pi, 0.99\pi]$, avoiding the flat-singularities. For instance, at grid point $\alpha_2 = 0$, the following steps were followed:

- All the polynomials in t_1 derived above were solved and the real values of $\alpha_1 \in]-\pi, \pi[$ were filtered out.
- The values of α_1 were arranged in increasing order along with the boundaries $-\pi, \pi$ as shown in Fig. 3a.
- One arbitrary point $(\alpha_1^*, 0)$ inside each of the interval was checked for wrench-feasibility and stability conditions. For wrench-feasibility, $(\underline{\Gamma_i} \leq G_i \leq \overline{\Gamma_i}), i = 1, 2$ were checked. For stability, firstly, the two forces that can be set to $F_{\max}$ at $(\alpha_1^*, 0)$, while the other forces remain within $[F_{\min}, F_{\max}]$ were identified. Then, all the forces were substituted into the stiffness matrix $\boldsymbol{K}_\alpha$ in Eq. (8) and its positive definiteness was evaluated. If the inspected point is both wrench-feasible and stable, the corresponding interval is feasible.
- All the feasible intervals are indicated with a tick mark in Fig. 3a, and the net bounding values of α_1 were found to be $[-1.20613, 1.20613]$ radians.

The above process is repeated for other discrete values of α_2 in Fig. 3b, and for α_1 in Fig. 3c. Since the bounding points are obtained by solving polynomials, it is not possible to miss out on any of these on the grid lines. Also, they are quite accurate with a very small residue (about 10^{-10} units) w.r.t. the original conditions.

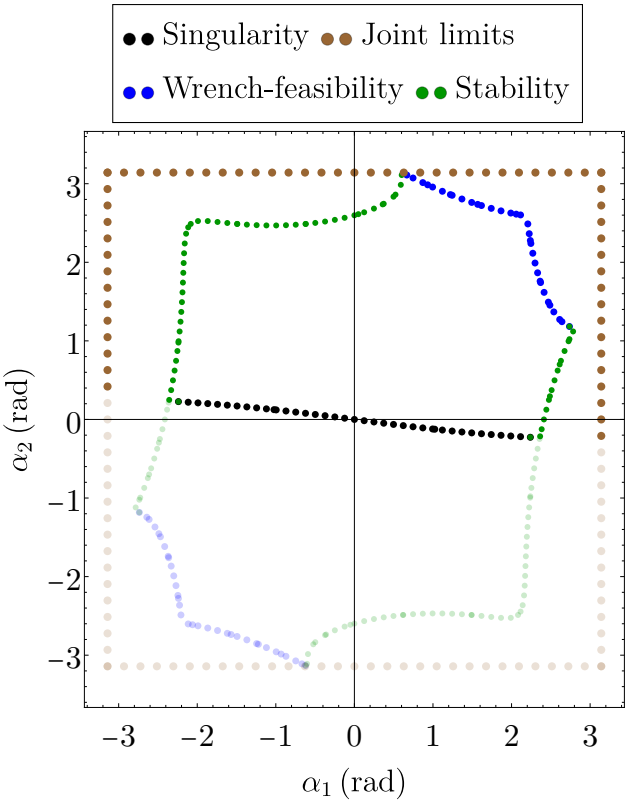

(a) Bounding points of SWFJ

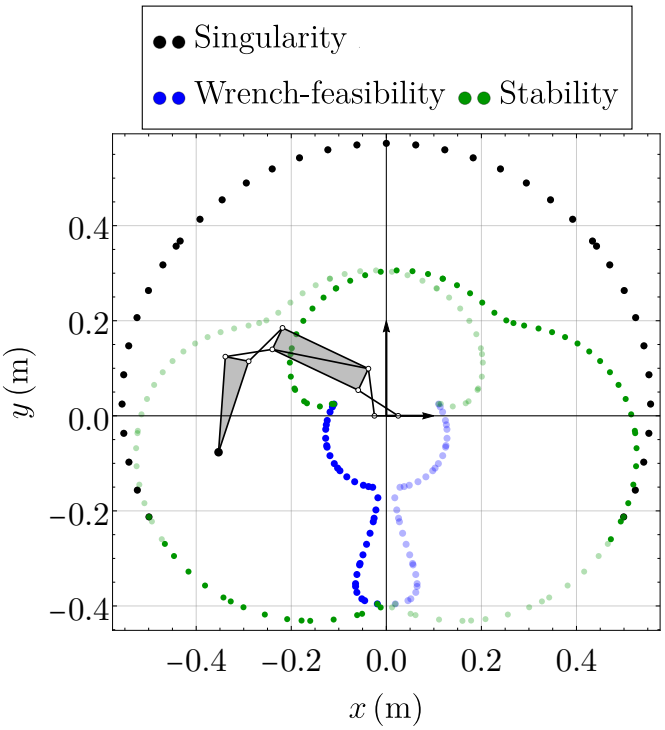

(b) Bounding points of the SWFW

Figure 4: Stable wrench-feasible joint space (left) and stable wrench-feasible workspace (right) of the 2-X manipulator when $b = 0.05$ m, $l = 0.1$ m, $a = 0.2$ m, $k_1 = 600$ N/m, $k_2 = 300$ N/m, $F_{\max} = 155$ N, $F_{\min} = 5$ N. In joint space (α_1, α_2), the points in region $\det(\boldsymbol{J}_x) > 0$ are shown in opaque style and those in $\det(\boldsymbol{J}_x) < 0$ region are shown in transparent style. Their maps in the task space are also shown in the same style for the sake of clarity.

Next, points on the singularity curve can be found using the condition in Eq. (3). It is possible to obtain polynomials out of the singularity condition and solve them to obtain the desired points along α_1 and α_2 grid lines, in a similar manner. The result is shown in Fig. 4a. All the points in the region $\det(\boldsymbol{J}_x) > 0$ are shown in opaque style while those in the region $\det(\boldsymbol{J}_x) < 0$ are shown in transparent style. These points have been mapped onto the task space using the kinematic equations in Eq. (1), to form the boundary points of the SWFW for this manipulator as shown in Fig. 4b. There are two regions in the SWFW bounded by the opaque and transparent points, each of which can be reached in one configuration. The top part where the two regions overlap can be reached in two configurations, and the central part around $(x = 0, y = 0)$ is unreachable.

6 Conclusion

A method to compute boundary points of the stable wrench-feasible workspace (SWFW) of a 2-X tensegrity manipulator driven by 4 cables was discussed. Firstly, it involves two 1-dimensional (D) scanning of the joints space. At each grid point, a set of univariate polynomials are solved to obtain the boundary points of the stable wrench-feasible joint space (SWFJ) accurately and quickly. These points are then mapped onto the task space of the manipulator along with the singularities, using the direct kinematic model, to obtain the corresponding bounding points of the SWFW of the manipulator. Since this is an automated process that can be implemented efficiently, it is suitable to be used in an optimal design process where several designs might be explored.

Appendix A Limiting condition(s) for positive definiteness for a (2×2) symmetric matrix

Consider a (2×2) real symmetric matrix $\boldsymbol{P}$ as shown below:

$$\boldsymbol{P} = \begin{pmatrix} p_{11} & p_{12} \\ p_{12} & p_{22} \end{pmatrix} \tag{27}$$

The conditions for its positive definiteness can be written in terms of its leading principal minors (see e.g., [4]) as follows:

$$\begin{cases} f_1 := p_{11} > 0 \\ f_2 := p_{11}p_{22} - p_{12}^2 > 0 \end{cases} \tag{28}$$

The limiting condition of stability is formed when one of the above inequalities becomes an equality, i.e., when ($f_1 = 0$ with $f_2 > 0$) or ($f_1 > 0$ with $f_2 = 0$). However, it is apparent that when $p_{11} = 0$, $f_2 = -p_{12}^2 < 0$ always . Thus, the only limiting condition for positive definiteness of $\boldsymbol{P}$ is given by ($f_2 = 0$ with $f_1 > 0$).

References

[1] M. Furet, P. Wenger, Kinetostatic analysis and actuation strategy of a planar tensegrity 2-X manipulator, Journal of Mechanisms and Robotics 11 (6) (2019) 060904. doi:10.1115/1.4044209.

[2] P. Wenger, M. Furet, Kinematic analysis of a planar manipulator with anti-parallelogram joints and offsets, in: J. Lenarčič, B. Siciliano (Eds.), Advances in Robot Kinematics 2020, Springer International Publishing, Cham, 2021, pp. 319–326.

[3] B. Fasquelle, P. Khanna, C. Chevallereau, D. Chablat, D. Creusot, S. Jolivet, P. Lemoine, P. Wenger, Identification and control of a 3-X cable-driven manipulator inspired from the bird's neck, Journal of Mechanisms and Robotics 14 (1) (2021) 011005. doi:10.1115/1.4051521.

[4] R. A. Horn, C. R. Johnson, Matrix Analysis, 2nd Edition, Cambridge University Press, 2012. doi:10.1017/9781139020411.